Journal of Molecular Spectroscopy 320 (2016) 33–38

Contents lists available at ScienceDirect

Journal of Molecular Spectroscopy

journal homepage: www.elsevier.com/locate/jms

The excited $J = 0$ $^1\Sigma_u^+$ levels of D_2: Measurements and *ab initio* quantum defect study

M. Glass-Maujean [a,*], Ch. Jungen [b,c], G.D. Dickenson [d], N. de Oliveira [e], W. Ubachs [d]

[a] Laboratoire d'Etudes du Rayonnement et de la Matière en Astrophysique et Atmosphères, UMR 8112, Sorbonne Universités, UPMC Univ. Paris 06/Observatoire de Paris/CNRS, F-75005 Paris, France
[b] Laboratoire Aimé Cotton du CNRS, Bâtiment 505, Université de Paris-Sud, F-91405 Orsay, France
[c] Department of Physics and Astronomy, University College London, London WC1E 6BT, United Kingdom
[d] Department of Physics and Astronomy, LaserLaB, VU University, De Boelelaan 1081, 1081 HV Amsterdam, The Netherlands
[e] Synchrotron Soleil, Orme des Merisiers, St. Aubin, BP 48, 91192 Gif sur Yvette, France

ARTICLE INFO

Article history:
Received 7 December 2015
In revised form 8 January 2016
Accepted 8 January 2016
Available online 11 January 2016

Keywords:
Vacuum ultraviolet Fourier-transform spectroscopy
Molecular deuterium
Analysis by multichannel quantum defect theory

ABSTRACT

The DESIRS beamline of the SOLEIL synchrotron facility, equipped with a vacuum ultraviolet Fourier-transform spectrometer has been used to measure $P(N'' = 1)$ $(N - N'' = -1)$ absorption transitions of the D_2 molecule. Some 44 *P*-lines were assigned and their transition frequencies determined up to excitation energies of 134,000 cm^{-1} above the ground state, thereby extending the earlier work by various authors, and considerably improving the spectral accuracy (<0.1 cm^{-1}). The assignments have been aided by first principles multichannel quantum defect theory (MQDT) calculations. These calculations also provide predictions of the autoionization widths of the upper levels which agree well with the observed resonance widths.

1. Introduction

Recently there has been renewed interest in the spectroscopy of the D_2 molecule because the isotopomers D_2 and H_2 are key molecules in the ongoing high-precision tests of quantum theory [1]. A detailed comparison of the spectroscopic properties of D_2 and H_2 must necessarily involve the study of non-adiabatic coupling of the electronic and nuclear degrees of freedom, a type of coupling which is strongly dependent on the nuclear mass.

D_2 has been less systematically studied than H_2. In the sixties and seventies of the preceding century only the lowest excited states that can be reached by photoabsorption have been studied in detail, namely the B, C, B' and D states, mainly in Herzberg's spectroscopy group at the National Research Council in Ottawa [2–5]. More recently the B, C, B' and D states have been reinvestigated at improved accuracy by classical emission spectroscopy [6,7], vacuum-ultraviolet (VUV) Fourier-transform absorption [8,9], and by Doppler-free VUV-laser excitation [10]. Higher electronic states of D_2 have been studied in photoabsorption in the seventies, in a single paper, as far as we are aware, by Takezawa and Tanaka [11] whose observations went up to ≈130,000 cm^{-1}.

Theoretical calculations on D_2 taking account of non-adiabatic effects in excited states began as early as 1977 when *ab initio* MQDT calculations of levels of the *B*, *C*, *D* and *B'* states based on the then best available quantum-chemical potential energy curves were published [12]. More recent studies are those of Refs. [6,7] where the coupled equations (CE) approach was used. A comparative study of the CE and MQDT methods as applied to the levels of the B' and C states was carried out in Ref. [13] a few years ago. The MQDT approach used in that work was similar to that employed in Ref. [12] but included various improvements and extensions such as the systematic inclusion of the energy dependence of the quantum defects (see Ref. [14]) and the calculation of transition intensities in addition to the level energies. The same approach was applied for the calculations contained in the very recent combined theoretical and experimental studies of excited $^1\Pi_u^-$ states of D_2 [15,16].

The purpose of the present paper is to extend the studies of Refs. [15,16] to the $N = 0$ excited levels of pure $^1\Sigma_u^+$ symmetry, which are investigated in absorption. These levels do not undergo

* Corresponding author.
E-mail addresses: michele.glass@upmc.fr (M. Glass-Maujean), christian.jungen@lac.u-psud.fr (Ch. Jungen).

http://dx.doi.org/10.1016/j.jms.2016.01.002
0022-2852/

any rotational-electronic non-adiabatic interactions, but they are significantly affected by vibrational-electronic (vibronic) coupling - much more so than their $^1\Pi_u^-$ counterparts. The MQDT calculations reported here have been carried out in exactly the same manner as those reported in Ref. [17] for the $N = 0$ $^1\Sigma_u^+$ levels of the H_2 isotopomer, except that the proton mass has been replaced by the deuteron mass in the computations. The reader is referred to that paper for all the details concerning the calculations. We shall use the calculated level positions and spectral line intensities for the further analysis of the absorption spectrum recorded at the SOLEIL synchrotron on the DESIRS beam line [8].

2. Experimental

The absorption spectrum of D_2 has been recorded using the Fourier-transform spectrometer installed on the DESIRS beamline at the SOLEIL synchrotron [18,19]. Before entering the spectrometer, the synchrotron radiation passes through a cell that is 10 cm long and contains the D_2 sample which is maintained at a quasi-static pressure of ≈0.1 mbar. The continuum background provided by the undulator corresponds approximately to a Gaussian of 7000 cm^{-1} width. The spectrum from 117,000 to 135,000 cm^{-1} has therefore been partitioned into four overlapping sections. The Fourier-transform spectrometer possesses its own internal calibration derived from the spatial step-size of the interferometer, which is controlled by a frequency stabilized He–Ne laser. Nevertheless small alignment errors may induce errors in the calibration that may vary from one recording to another. De Lange et al. [9] introduced corrections for the different energy intervals under investigation, which account for the small deviations in the travel of the moving mirror. By applying these derived corrections it is possible to improve the accuracy of the measurements, and, for higher energies for which no corrections have been derived, it is possible to extrapolate these corrections and again improve the accuracy of the measurements. This procedure however induces a residual error which increases as the energy increases [15].

The continuum background has been fitted to a Gaussian and Beer–Lambert's law applied to obtain a signal proportional to the absorption cross section. A section of this quantity is plotted in Fig. 1 along with the calculated $P(1)$ transitions and their assignments. The individual observed peaks thus obtained have been fitted to Gaussians, from which the natural widths were determined as follows.

Each observed absorption transition represents the result of the convolution of three effects: (i) the apparatus function which has the form of a sinc function, (ii) the Doppler width which is a Gaussian, and (iii) the natural width which typically corresponds to a Lorentzian. As the Doppler width (0.4 cm^{-1}) is much larger than the apparatus function (0.16 cm^{-1}), the convolution of these two functions is well represented by a single Gaussian function of width 0.4 or 0.5 cm^{-1} depending on the spectral recording considered. We have verified this point by test calculations made by measuring the effective widths of lines known to produce fluorescence radiation, and whose natural widths therefore are far less than the Doppler width and the instrument width [16]. Next, we have calculated for each transition the line profile resulting from the convolution of the known Gaussian representing the effective Doppler width and an assumed Lorentzian profile representing the natural width. This profile was fitted itself by a Gaussian, which was then compared to the experimentally determined effective width. For each transition the assumed natural width was then varied until the observed effective width could be reproduced. The uncertainty of the natural width thus determined was taken to be three times the uncertainty obtained in the fit. Despite the high spectral resolution achieved in this experiment, we have found that many transitions are not completely resolved so that we had to represent the profiles by several overlapping Gaussians. The uncertainty of the natural width determination in these cases is substantially larger.

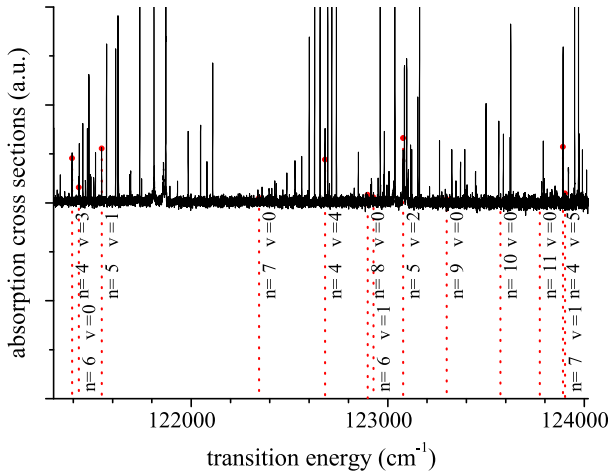

Fig. 1. Absorption cross section (in arbitrary units) of D_2 between 121,400 and 124,000 cm^{-1} taken at the DESIRS beamline of the SOLEIL synchrotron. Calculated $P(1)$ transitions leading to $np\sigma, v, N = 0$ Rydberg levels are indicated by filled circles (red online). Their intensities have been adjusted to the experiment by a global adjustment factor. (For interpretation of the references to colour in this figure legend, the reader is referred to the web version of this article.)

3. Calculations

As has already been stated the calculations have been carried out in exactly the same fashion as in our previous paper on the $P(1)$ transitions H_2 [17], except that the reduced nuclear mass and the value of the Rydberg constant have been adapted to the D_2 molecule. The approach assumes that the Rydberg spectrum corresponds to excitation of a single electron which may be described by a single partial wave, $\ell = 1$ which yields $np\sigma$ and $np\pi$ Rydberg configurations. Higher partial waves and doubly excited configurations are not explicitly taken into account. However the quantum defect functions derived from *ab initio* potential energy curves account [20,21] for the effect of such configurations in an effective manner (cf. Ref. [17] for details and the general comments made in Ref. [12]). In practice, two sets of calculations have been carried out. In the first set of calculations all open ionization channels have been artificially removed so that a spectrum of discrete lines was obtained which was used for the purposes of spectral assignments and from which the line intensities were obtained. In the second set of calculations the open ionization channels were retained so that the MQDT calculations yielded a continuous spectral intensity distribution from which, via a fit to a Lorentzian shape, the width for each autoionization resonance could be extracted. Unlike in the previous Ref. [17] we have neglected the effect of predissociation in the present work as it significantly affects only few of the observed upper levels (cf. the discussions in Section 4.2 below and in the following paper [22]).

4. Results

The present results are summarized in Table 1. We discuss the various aspects consecutively.

4.1. Energy levels

We have been able to assign 44 $P(1)$ lines unambiguously in the range 117,300–134,300 cm^{-1}. These correspond to upper level

Table 1
$P(1)$ transitions in the photoabsorption spectrum of the D_2 molecule.

state	v	ν/c obs[a]	±[b]	obs-calc	Γ (obs)[c]	±[b]	Γ_i (calc)[d]
$4p\sigma$	0	117137.40	(0.04)	-0.53	0.00	(0.16)	
$4p\sigma$	1	118628.25	(0.03)	-0.51	0.00	(0.16)	
$5p\sigma$	0	*119964.61*					
$4p\sigma$	2	120052.72	(0.04)	-0.51	0.00	(0.15)	
$4p\sigma$	3	121393.89	(0.03)	-0.28	0.01	(0.15)	
$6p\sigma$	0	121427.85	(0.04)	-0.07	0.00	(0.18)	
$5p\sigma$	1	121544.22	(0.04)	-0.62	0.01	(0.15)	
$7p\sigma$	0	*122344.84*					
$4p\sigma$	4	122680.82	(0.03)	-0.01	0.02	(0.15)	
$8p\sigma$	0	*122897.97*					
$6p\sigma$	1	122927.33	(0.07)	-0.10	0.00	(0.19)	
$5p\sigma$	2	123077.98	(0.05)	-0.70	0.15	(0.16)	
$9p\sigma$	0	*123300.46*					
$4p\sigma$	5	123890.95	(0.07)	-0.32	0.09	(0.15)	
$7p\sigma$	1	123901.50	(0.08)	-0.22	0.00	(0.24)	
$5p\sigma$	3	124325.74	(0.88)	-0.08	0.38	(0.92)	
$8p\sigma$	1	*124468.14*					
$6p\sigma$	2	124569.22	(0.04)	-0.64	0.00	(0.15)	
$9p\sigma$	1	*124870.46*					2.9
$4p\sigma$	6	125026.34	(0.05)	-0.34	0.00	(0.15)	0.000002
$7p\sigma$	2	125404.49	(0.09)	0.00	0.37	(0.17)	0.17
$5p\sigma$	4	125667.90	(0.05)	0.03	0.00	(0.15)	0.00029
$6p\sigma$	3	125930.93	(0.05)	-0.30	0.12	(0.16)	0.003
$8p\sigma$	2	126025.17	(0.04)	-0.39	0.09	(0.15)	0.013
$4p\sigma$	7	126086.71	(0.04)	-0.33	0.04	(0.15)	0.0004
$9p\sigma$	2	126372.69	(0.69)	-2.02	5.90	(3.62)	6.2
$7p\sigma$	3	126816.55	(0.10)	-0.20	0.06	(0.23)	0.27
$5p\sigma$	5	126937.56	(0.06)	0.04	0.07	(0.16)	0.001
$4p\sigma$	8	127071.15	(0.04)	-0.37	0.05	(0.16)	0.0002
$6p\sigma$	4	127310.23	(0.05)	-0.54	0.06	(0.15)	0.032
$8p\sigma$	3	127443.05	(0.04)	-0.28	0.00	(0.15)	0.014
$9p\sigma$	3	*127814.57*					8.9
$4p\sigma$	9	127968.82	(0.06)	-0.35	0.08	(0.16)	0.0001
$5p\sigma$	6	128153.20	(0.05)	-0.12	0.12	(0.15)	0.084
$7p\sigma$	4	*128196.95*					0.34
$6p\sigma$	5	128616.05	(0.04)	-0.66	0.10	(0.15)	0.045
$4p\sigma$	10	128813.74	(0.05)	-0.48	0.07	(0.15)	0.031
$8p\sigma$	4	128824.86	(0.08)	-0.01	0.75	(0.19)	0.73
$9p\sigma$	4	129191.62	(0.05)	-0.15	0.00	(0.16)	0.028
$5p\sigma$	7	129289.41	(0.04)	-0.20	0.05	(0.15)	0.057
$7p\sigma$	5	*129518.48*					4.5
$4p\sigma$	11	129596.58	(0.06)	0.02	0.16	(0.16)	0.001
$6p\sigma$	6	129861.94	(0.07)	-0.68	0.84	(0.17)	0.65
$8p\sigma$	5	130112.83	(0.10)	-0.45	0.18	(0.20)	0.28
$4p\sigma$	12	*130307.27*					0.001
$5p\sigma$	8	130376.78	(0.04)	-0.63	0.03	(0.15)	0.002
$9p\sigma$	5	*130507.60*					0.18
$7p\sigma$	6	*130707.23*					0.25
$4p\sigma$	13	130992.06	(0.12)	0.66	0.30	(0.30)	0.003
$6p\sigma$	7	131049.05	(0.93)	-0.96	2.60	(1.45)	2.0
$5p\sigma$	9	131374.69	(0.13)	-0.40	0.63	(0.32)	1.5
$8p\sigma$	6	131403.70	(0.55)	0.03	1.70	(0.92)	2.1
$9p\sigma$	6	*131743.46*					0.029
$7p\sigma$	7	*131885.61*					0.003
$6p\sigma$	8	132169.03	(0.20)	0.73	0.56	(0.48)	1.3
$5p\sigma$	10	132336.69	(0.05)	1.48	0.05	(0.15)	0.30
$8p\sigma$	7	132583.83	(0.38)	0.61	3.60	(2.34)	2.5
$6p\sigma$	9	*133325.39*					8.2
$6p\sigma$	10	134317.06	(0.08)	-1.46	0.82	(0.18)	0.60

Values in italics are calculated transition energies, given when there is no corresponding observation.
The positions of the upper state energy levels above the $v''=0, N''=0$ ground state level are obtained by adding the ground-state rotational energy 59.78 cm^{-1} ($N''=1$) [1] to the transition energy.
[a] Transition energy in cm^{-1}.
[b] Uncertainty in cm^{-1}.
[c] Observed line width in cm^{-1}.
[d] Calculated ionization width in cm^{-1}.

$np\sigma\ ^1\Sigma_u^+$ with $n \geqslant 4$. The $2p\sigma B\ ^1\Sigma_u^+$ and $3p\sigma B'\ ^1\Sigma_u^+$ states have been studied previously and their discrete level structure lies at lower energies than we consider here [9]. The uncertainty of the energy levels has been taken as three times the statistical error plus the uncertainty of the calibration (up to 0.04 cm^{-1}). In the case of very weak lines an additional uncertainty arises which amounts to 0.07 cm^{-1} and corresponds to the interval of the noise wiggles (i.e. the energy difference between successive wiggles) present in the recordings.

The deviations observed–calculated are generally less than 1 cm^{-1}, but are clearly larger than the experimental uncertainty and therefore reflect the short-comings of our calculations. The

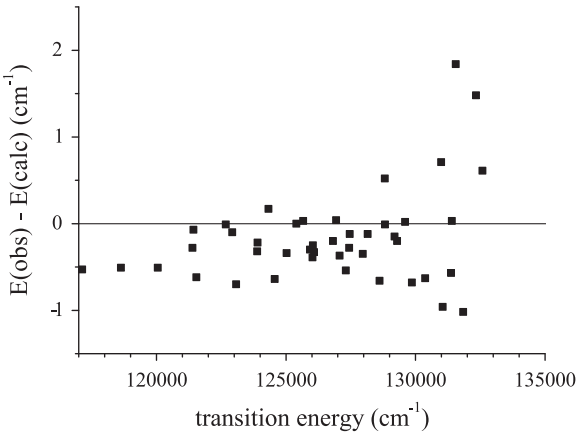

Fig. 2. Deviations observed–calculated for the $P(1)$ transitions assigned in the D_2 absorption, plotted versus the transition energy.

histogram of the deviations observed–calculated corresponds in a good approximation to a Gaussian centered at -0.29 ± 0.03 cm^{-1} and a width of 0.6 cm^{-1}. Fig. 2 is a plot of these deviations versus the transition energy which shows that the accuracy of the calculations deteriorates as the energy increases. The higher excitation energies lead to higher electronic as well as higher vibrational excitation. In higher vibrational levels the molecule explores larger internuclear distances, where the assumptions underlying the theoretical approach begin to break down. Specifically, the $B''\bar{B}\ ^1\Sigma_u^+$ state possesses a potential maximum near $R \approx 6$ a.u. at an energy $\approx$130,000 cm^{-1} [5,23], which is disregarded in our approach, but whose effects clearly show up in the plot of Fig. 2. A fuller treatment would require explicit inclusion of core-excited Rydberg channels and of the long-range H^++H^- ion-pair channel. These developments are outside of the scope of the present paper.

The intensities of the $np\sigma$ $P(1)$ transitions are expected to decrease with increasing principal quantum number n in accordance with the n^{-3} Rydberg scaling law. This is true overall, but locally the effects of vibronic interseries perturbations disrupt the regular decrease. At the same time the autoionization widths are rather substantial in the pure $^1\Sigma_u^+$ symmetry upper levels of the $P(1)$ transitions - several cm^{-1} in some cases - with the result that for $n \geqslant 10$ the resonances tend to merge into the background continuum and cannot be detected in our experiment. Further, as v increases, the density of states increases while the line intensities strongly decrease for $v \geqslant 4$ due to unfavorable Franck–Condon factors. The widths also tend to increase. As a result, again, definitive assignments become more difficult at higher energies. Nevertheless it has been possible to follow the upper levels of $4p\sigma$ up to $v = 13, 5p\sigma$ and $6p\sigma$ up to $v = 10, 7p\sigma$ up to $v = 3, 8p\sigma$ up to $v = 7$, and $9p\sigma$ up to $v = 4$, respectively.

The $P(1)$ transitions to $4p\sigma, v = 0 - 9$ have previously been observed and assigned by Takezawa and Tanaka [11]. We have remeasured them here with higher accuracy and extended the vibration progression to $v = 13$. Similarly, Takezawa and Tanaka had observed the $5p\sigma$ and $6p\sigma$ progressions up to $v = 4$ and $v = 3$, respectively, whereas we have remeasured all of these transitions and extended the assignments up to $v = 10$. It turns out that the $5p\sigma, v, N = 0$ and $6p\sigma, v - 1, N = 0$ levels are completely mixed by $\Delta v = 1$ vibronic interaction for $v = 3$ and $v = 4$. By labeling each level according to the largest channel contribution given by the MQDT calculation we find that we have to invert the assignments made by Takezawa and Tanaka [11], by formally assigning the $P(1)$ transition at 124325.7 cm^{-1} to $5p\sigma, v = 3 \leftarrow X, v'' = 0$ instead of $6p\sigma, v = 2 \leftarrow X, v'' = 0$, and the transition at 125667.9 cm^{-1} to $5p\sigma, v = 4 \leftarrow X, v'' = 0$ instead of $6p\sigma, v = 3 \leftarrow X, v'' = 0$, and changing the assignments of the transitions at 124569.2 cm^{-1} and 125930.9 cm^{-1} accordingly. Recall however that these assignments to specific upper levels $np\sigma, v$ have only a limited meaning and are useful mainly for book-keeping purposes. It is the full MQDT calculation which accounts for the vibronic interactions and produces mixed states that allows the spectrum to be analyzed. Another reassignment concerns the $P(1)$ $4p\sigma, v = 9 \leftarrow X, v'' = 0$ transition which is identified here as corresponding to the line observed at 127968.2 cm^{-1}, whereas previously [11] it had been assumed to be blended by the $R(0)$ $4p\pi, v = 7 \leftarrow v'' = 0$ transition that appears at 127974.2 cm^{-1}, i.e. about 6 cm^{-1} higher.

Overall, out of 18 $P(1)$ line assignments corresponding to $4 - 6p\sigma$ published previously [11], 3 have been reassigned, one has been invalidated ($4p\sigma, v = 9$), while the remaining transitions have been remeasured here with higher accuracy. $5p\sigma, v = 0$ is an exception as it is too weak in our spectra to be unambiguously assigned. 26 $P(1)$ transitions $np\sigma$ with $n = 4 - 9$ are reported here for the first time.

4.2. Widths

The natural decay widths of the upper levels of the $P(1)$ transitions have been determined as described in Section 2 and are included in Table 1. The uncertainties given in Table 1 correspond to three times the 1σ statistical errors due to the measurement of each resonance and to the apparatus function ($\approx$0.15 cm^{-1}). These values are compared in Table 1 and Fig. 3 with the calculated ionization widths. In most cases the calculated width is less than the uncertainty of the measurement, which therefore provides an upper limit for the natural width.

All $4p\sigma$ resonances are calculated to have widths less than the experimental uncertainty. Exceptions arise for $v = 11$ and $v = 13$ where the measured values are larger than calculated. We suspect that these widths are due mainly to dissociation, a decay channel that we have not included in our calculations. Indeed we know from the study of H_2 that these levels primarily decay via predissociation [24]. Fig. 3 shows that while the experimental widths of the $5p\sigma$ levels with v values around 6 agree with the calculated ionization widths in the sense specified above, there is marked disagreement for $v = 3$ and $v = 9$. The line intensity in the latter case is quite weak and hence the experimental determination has a large uncertainty, but nevertheless the calculated ionization width is distinctly larger than the observed value, a fact that is not understood at this stage. The line widths of the $6p\sigma$ progressions again agree with the calculations. The large calculated width of $v = 9$ is to be noted - however it has proved impossible to locate the corresponding transition in the experimental spectrum. The few transitions to $7p\sigma$ levels that have been identified experimentally, up to $v = 3$ only, yield widths that are again in line with the calculations. The same is true for the few observations that we have made in the $8p\sigma$ progression, cf. Fig. 3.

Only two transitions belonging to the $9p\sigma$ progression have been observed, namely $v = 2$ and $v = 4$. The observed and calculated large widths for $v = 2$ are in nice agreement, 5.9 ± 3.6 and 6.2 cm^{-1}, respectively, and this is also the case for the contrastingly small $v = 4$ widths: 0.00 ± 0.16 and 0.03 cm^{-1}, respectively. The latter case is interesting as the $9p\sigma, v = 4, N = 0$ level is part of a 'complex' resonance [25], as it is immersed in the dense manifold of Rydberg levels $np\sigma, v = 3$ with $n \approx 43$ with which it interacts. These are spaced by about 2.8 cm^{-1} and have very small ionization widths in such a way that the present experiment is able to resolve the comb-like fine structure of the 'complex' resonance, see Fig. 4. For this reason the observed value for the width given in Table 1 is the genuine width of the $9p\sigma, v = 4$ interloper and does not reflect the width of the whole group of interacting levels.

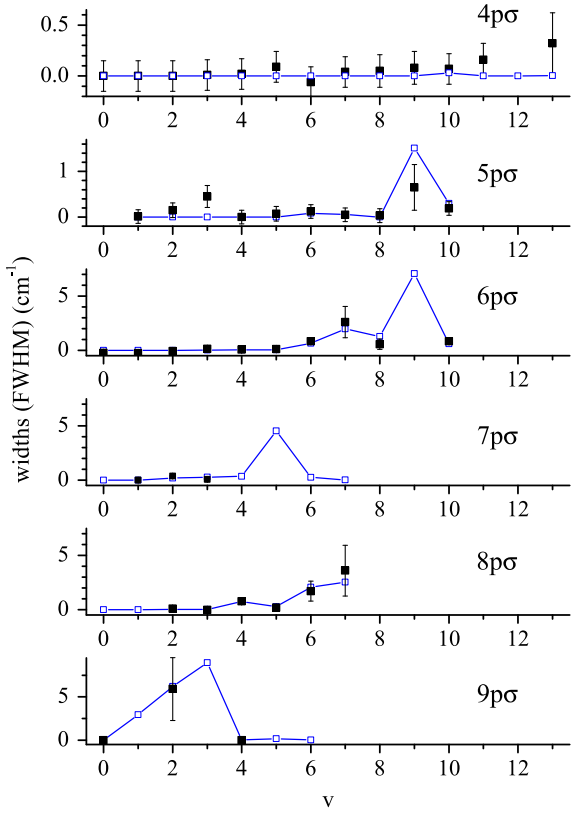

Fig. 3. Observed (black filled squares) and calculated (open blue squares) natural widths of $P(1)$ transitions assigned in the D_2 absorption spectrum, plotted versus the vibrational quantum number. The calculated widths correspond to the ionization partial widths obtained from the MQDT calculations. (For interpretation of the references to colour in this figure legend, the reader is referred to the web version of this article.)

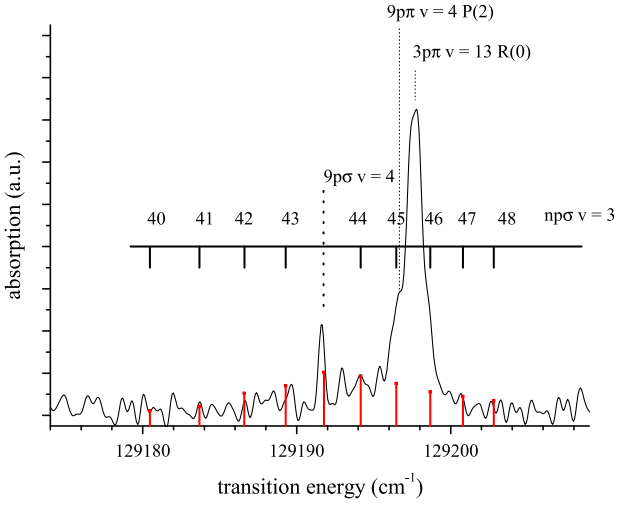

Fig. 4. Section of the absorption spectrum of D_2 near 129,200 cm^{-1} showing the $9p\sigma, v = 4, N = 0$ resonance immersed in the $np\sigma, v = 3, N = 0$ Rydberg series with $n \approx 43$.

In conclusion, it appears that the observed widths of the $P(1)$ transitions are for the most part due to autoionization, whereas predissociation contributes significantly only for $n = 4$ ($4p\sigma$ progression). The ionization widths of all the upper levels with $n \leqslant 8$ are basically quite small as they cannot proceed via the $\Delta v = 1$ propensity rule since the $v - 1$ ionization continuum is closed for this class of upper levels. Their widths are erratic as they may be enhanced only by the accidental local perturbations, which involve levels that are able to ionize via the preferred $\Delta v = 1$ ionization route. These perturbing levels then play the role of 'doorway' states as they are known in non-radiative transitions in large molecules or in nuclear reactions [26,27].

5. Summary and conclusion

We have observed the VUV Fourier-transform absorption spectrum of D_2 and analyzed in the present paper the $P(1)$ transitions with the help of first-principles MQDT calculations. The lower states correspond to $X^1\Sigma_g^+, v'' = 0, N'' = 1$, while the $N = 0$ upper states of these transitions have positive total parity and pure $^1\Sigma_u^+$ electronic symmetry. We have identified 44 such transitions with an experimental uncertainty of better than 0.1 cm^{-1}. The upper states correspond to Rydberg series $np\sigma$ with $4 \leqslant n \leqslant 9$. 18 transitions have been observed previously but are determined here with improved accuracy, while the remaining ones are reported here for the first time. On the basis of our calculations we have revised a few previous assignments. The observed and calculated line frequencies agree to within 0.3 cm^{-1} on the average. The ionization widths have also been evaluated and agree fairly well with the natural widths extracted from the experimental spectra. Overall, however, the agreement between experiment and theory deteriorates noticeably as the energy increases and levels are excited whose vibrational motion explores internuclear distances up to and beyond ≈5 a.u..

Acknowledgments

The authors thank D. Joyeux for his help in the data acquisition on the FTS and L. Nahon for his constant support. Ch. J. thanks the Miescher Foundation (Basel, Switzerland) for partial support.

References

[1] J. Liu, D. Sprecher, Ch. Jungen, W. Ubachs, F. Merkt, J. Chem. Phys. 132 (2010) 154301-1–154301-11.
[2] G. Herzberg, A. Monfils, J. Mol. Spectrosc. 5 (1960) 482–498.
[3] A. Monfils, Bull. Acad. Roy. Belg. (Sciences) 48 (1965) 482–489.
[4] A. Monfils, J. Mol. Spectrosc. 15 (1965) 265–307.
[5] I. Dabrowski, G. Herzberg, Can. J. Phys. 52 (1974) 1110–1136.
[6] M. Roudjane, F. Launay, W.-Ü.L. Tchang Brillet, J. Chem. Phys. 125 (2006) 214305-1–214305-9.
[7] W.-Ü.L. Tchang Brillet, M. Roudjane, F. Launay, J. Chem. Phys. 127 (2007) 054307-1–054307-6.
[8] G.D. Dickenson, T.I. Ivanov, W. Ubachs, M. Roudjane, N. de Oliveira, D. Joyeux, L. Nahon, W.-Ü.L. Tchang-Brillet, M. Glass-Maujean, H. Schmoranzer, A. Knie, S. Kübler, A. Ehresmann, Mol. Phys. 109 (2011) 2693–2708.
[9] A. de Lange, G.D. Dickenson, E.J. Salumbides, W. Ubachs, N. de Oliveira, D. Joyeux, L. Nahon, J. Chem. Phys. 136 (2012) 234310-1–234310-9.
[10] M. Roudjane, T.I. Ivanov, M.O. Vieitez, C.A. de Lange, W.-Ü.L. Tchang-Brillet, W. Ubachs, Mol. Phys. 106 (2008) 1193–1197.
[11] S. Takezawa, Y. Tanaka, J. Mol. Spectrosc. 54 (1975) 379–401.
[12] Ch. Jungen, O. Atabek, J. Chem. Phys. 66 (1977) 5584–5609.
[13] M. Glass-Maujean, Ch. Jungen, M. Roudjane, W.-Ü.L. Tchang-Brillet, J. Chem. Phys. 134 (2011) 204305-1–204305-14.
[14] Ch. Jungen, Elements of quantum defect theory, in: M. Quack, F. Merkt (Eds.), Handbook of High Resolution Spectroscopy, Wiley, Chichester and New York, 2011.
[15] M. Glass-Maujean, Ch. Jungen, G.D. Dickenson, W. Ubachs, N. de Oliveira, D. Joyeux, L. Nahon, J. Mol. Spectrosc. 315 (2015) 147–154.
[16] M. Glass-Maujean, A.-M. Vasserot, Ch. Jungen, H. Schmoranzer, A. Knie, S. Kübler, A. Ehresmann, J. Mol. Spectrosc. 315 (2015) 155–171.
[17] M. Glass-Maujean, Ch. Jungen, H. Schmoranzer, I. Haar, A. Knie, P. Reiss, A. Ehresmann, J. Chem. Phys. 135 (2011) 144302-1–144302-12.
[18] N. de Oliveira, D. Joyeux, D. Phalippou, J.-C. Rodier, F. Polack, M. Vervloet, L. Nahon, Rev. Sci. Instrum. 80 (2009) 043101-1–043101-14.
[19] N. de Oliveira, M. Roudjane, D. Joyeux, D. Phalippou, J.-C. Rodier, L. Nahon, Nat. Photon. 5 (2011) 149–153.
[20] L. Wolniewicz, G. Staszewska, J. Mol. Spectrosc. 220 (2003) 45–51.
[21] <http://fizyka.umk.pl/ftp/pub/publications/ifiz/luwo>, 2013.

[22] M. Glass-Maujean, A.-M. Vasserot, Ch. Jungen, H. Schmoranzer, A. Knie, S. Kübler, A. Ehresmann, J. Mol. Spectrosc. (2016), http://dx.doi.org/10.1016./j.jms.2016.01.003.
[23] W. Kołos, J. Mol. Spectrosc. 62 (1976) 429–441.
[24] M. Glass-Maujean, S. Klumpp, L. Werner, A. Ehresmann, H. Schmoranzer, J. Chem. Phys. 126 (2007) 144303-1–144303-8.
[25] Ch. Jungen, M. Raoult, Farad. Disc. Chem. Soc. 71 (1981) 253–271.
[26] A.J. Fleisher, R.G. Byrd, D.P. Zaleski, B.H. Pate, D.W. Pratt, J. Phys. Chem. B 117 (2013) 4231–4240.
[27] H. Feshbach, Rev. Mod. Phys. 46 (1974) 1–5.